CHARACTERIZATION OF THE CHEMISTRY AT THE ANODE AND CATHODE IN THE Li/SO_2 BATTERY SYSTEM

WILLIAM P. KILROY and CHARLES R. ANDERSON
Naval Surface Weapons Center, White Oak, Silver Spring, MD 20910 (U.S.A.)
(Received June 7, 1982)

Summary

The discharge product of Li/SO_2 cells discharged at 25 °C at 1 - 2 mA/cm^2 was quantitatively analyzed for sulfite, thiosulfate, and dithionite. Analysis of the lithium anodes of commercial Li/SO_2 batteries by XPS, SAM, SEM, and mass spectroscopy techniques determined the passive film chemistry to be complex, but generally dominated by lithium sulfite and sulfate formation. The anode microstructure and chemistry is inhomogeneous and sensitively dependent upon the state of discharge and the discharge temperature.

Introduction

To date, two areas of chemistry in the Li/SO_2 battery system have never been unequivocally resolved; namely, the nature of the cathodic discharge product and the nature of the anodic film. The cathode product has been assumed to be dithionite, based on qualitative studies [1] and the numerous voltammetric investigations often performed under conditions dissimilar to those in commercial cells. This paper reports quantitative analysis of the cathode product for the SO_2 system discharged at 25 °C.

Similarly, the proposed [2, 3] nature of the passivating film on lithium has never been confirmed. This film formed at the interface of the lithium with the electrolyte-depolarizer permits the Li/SO_2 cell to function by imparting a kinetic stability to an otherwise thermodynamically unstable system. This passivation may be either (a) "chemical" as occurs in undischarged cells and is characterized by a voltage delay or (b) "anodic" as occurs when the lithium anode polarizes leaving lithium incompletely oxidized. In either case, degradation of this film may lead to safety hazards *via* spontaneous chemical reactions. Both the performance (chemical and anodic passivation) and the reported safety incidences can best be assessed by a better understanding of the fundamental processes involved in the formation of this passivating layer. This paper also reports the chemical and structural nature of this film as found in a commercial, hermetically

0378-7753/83/0000-0000/$03.00

sealed cell of the acetonitrile (AN)/LiBr/SO_2 system using the techniques of X-ray photoelectron spectroscopy (XPS), mass spectroscopy of the products of pumped, heated, and ion bombarded lithium anodes, scanning Auger microprobe (SAM), and secondary electron microscopy (SEM).

Experimental

Cells

Chemical analyses of discharged cathodes were performed using both research and commercial cells. The research cell was a pressurized vessel containing an electrode assembly filled with Honeywell commercial SO_2 reserve ($LiAsF_6$) or active (LiBr) electrolyte. The electrode, assembled under argon, consisted of either one or two pieces of 80% Shawinigan carbon black–20% Teflon (previously dried at 150 °C under vacuum for two days) placed between two pieces of lithium, separated from them by polypropylene, and bound together between two pieces of glass with stainless steel wire. The commercial cells were hermetically sealed 1/2 A size cells.

Chemical analysis

Commercial 1/2 A cells were discharged at 25 °C at a constant current of 40 mA (0.77 mA/cm^2) to a 2.0 volt cutoff. Research cells were discharged under a variety of conditions at 25 °C. The cells were dismantled or cut open under argon. The carbon cathodes were ground with a mortar and pestle, placed in a beaker in a vacuum desiccator and evacuated overnight. The discharged anodes and cathodes were added separately and/or together to a cold, de-aerated 0.1M sodium hydroxide solution. The mixture was maintained under argon and stirred for about five hours or until constant results were achieved. Analysis was performed by a procedure previously described [4]. An undischarged cell was similarly analyzed and was used as a blank to correct for background components.

Surface analysis

Surface analysis was performed on the lithium anodes of commercial cells which were undischarged or discharged at 0.77 mA/cm^2 of lithium anode at −30, 24, and 70 °C.

The cells were allowed to equilibrate for one hour at the appropriate temperature prior to discharge. The cells discharged at −30 °C were discharged until the voltage dropped to 0.1 V. The cell discharged at 24 °C had a discharge cut-off voltage of 2.6 V, while the 70 °C discharged cells had a cut-off voltage of 2.0 V. The cells were immediately transferred to an argon glove box, cut open, and the unwashed lithium anodes were placed in a vacuum desiccator which was evacuated by a mechanical pump for one-half to one hour to remove SO_2 and AN vapors before transfer in the vacuum desiccator to a helium glove box. The helium glove box was equipped with an attached vacuum chamber having a cryogenic, molecular sieve pump. The

fast insertion probe and chamber of a Kratos ES300 XPS system, after suitable modification, were transferred under vacuum to the helium glove box and bolted onto the attached vacuum system which was then evacuated. The sample probe was pushed into the glove box where the sample mounting was accomplished for XPS analysis. The probe was then withdrawn back into the modified Kratos fast insertion chamber and its ball valve was closed. The sample was then transferred under helium to the XPS system, reattached, and evacuated.

Samples for SAM analysis were mounted on the fast transfer 60° angle stages of the Physical Electronics Division of Perkin-Elmer 590A SAM fast sample insertion system. The sample transfer stage was then double bottled under helium and transferred to the SAM system. The transfer probe was withdrawn to the load position and N_2 gas was allowed to flow at a high rate through the insertion vacuum interlock chamber and out over the end of the sample probe. Within about 5 s, the transfer stage was removed from the inside bottle, placed on the probe, and the probe was pushed into the fast insertion vacuum interlock and evacuation started.

Samples for SEM analysis were mounted on sample holders in the helium glove box, double-bottled, and transferred to a gold sputter deposition vacuum system, which exposed them to air for less then 10 s. About 300 Å of gold was then argon sputtered onto them and they were again, in this protected state, exposed to air for about 10 s by the transfer to the SEM.

During XPS and SAM analysis pressures were generally in the 10^{-10} Torr range and sometimes the high 10^{-11} Torr range. XPS analysis was performed using Mg Kα X-ray radiation. The lithium anode samples were XPS analyzed at the as-transferred surface, after argon ion bombardment and after heating the samples to 100 °C. In most cases, the high resolution spectra were recorded as a function of time to observe the effects, if any, due to X-ray damage and time. The SAM analyses were performed with a rastered beam of 50 nA at 3 keV. The SEM electron photomicrographs were made on an AMR 1000A at sub-nanoamp currents. All samples were analyzed at normal temperature (~23 °C), though as noted, some were later heated in the XPS system.

Mass spectroscopy observations were made with a Granville-Phillips SpectraScan 750 quadrupole mass spectrometer mounted in direct line-of-sight of the sample in the analysis chamber of the XPS system. Argon ion bombardment and heating of the sample could also be accomplished with the sample facing the mass spectrometer bottle-mounted head.

Results and discussion

Chemical analysis

The data in Table 1 summarize chemical analyses performed on research and commercial cells discharged at 25 °C to a 0.1 V cutoff. The research cells differed from the commercial cells in that the electrodes were

TABLE 1

Chemical analysis of Li/SO_2 cells discharged at 25 °C to a 0.1 volt cutoff

Run*	Current density (ma/cm^2)	Coulombs passed	$S_2O_4^{2-}$ (mmoles)	$S_2O_3^{2-}$	SO_3^{2-}	Coulombs ($S_2O_4^{2-}$)	as $S_2O_4^{2-}$ (%)
1	—	1442	7.11	0.18	1.28	1372	95.1
2	1.0	1203	6.20	0.00	0.00	1197	99.5
3	2.0	1788	8.99	0.00	0.1	1735	97.0
4	1.5	1138	5.99	0.00	0.00	1156	101.6
5	0.77	3170	16.59	—	—	3202	101.0

*Runs 1 - 3 $Li/LiAsF_6/SO_2$ (commercial electrolyte in a pressurized research cell); runs 4, 5 $Li/LiBr/SO_2$; run 5, commercial 1/2 A cell.

flooded with excess electrolyte and were contained in a glass vessel. Run 1 differed from the other runs in that the cell was discharged under a 200 Ω load and the carbon cathodes were not dried prior to assembly. Additional studies need to be performed to determine if the moisture present in the carbon may account for the sulfite found. The sulfite found far exceeds the stoichiometric amount predicted from the thermal disproportionation of the dithionite [5]. Constant current discharge performed on research cells (Runs 2 - 4) containing dried cathodes, and on a commercial 1/2 A size cell (run 5), show that the discharge product is principally lithium dithionite, provided the discharge occurs at low current densities and at normal temperature. Studies performed (a) on cells discharged at high current densities, and (b) at temperatures other than normal temperature, revealed that dithionite is not the sole product found.

SEM

Electron photomicrographs of the lithium anodes discharged at −30, 24, and 70 °C are shown in Fig. 1. By contrast, the surface of the undischarged lithium is uniform with only modest roughening. At 24 °C, lithium was removed preferentially from the anode at a small number of spots. At these spots, large craters formed, such as that of Fig. 1(d), which created a hole through the anode. The edge of this crater is shown in Fig. 1(e) and is seen to have a moderately high surface area, in many areas covered with small platelets. Outside the craters, the initial chemical passive film has nonetheless been highly modified by discharge. This anodic passive film takes several forms at 24 °C including the tube-building region of Fig. 1(f). In this region the Li^+ transport appears to be occurring preferentially along channels of about 0.5 μm dia. Some of these lithium ions apparently form reaction products with the electrolyte and products already dissolved in it, and these new products form the walls of tubes around the ion transport channels, with many collapsing in time. Again, many small platelets are observed in this region.

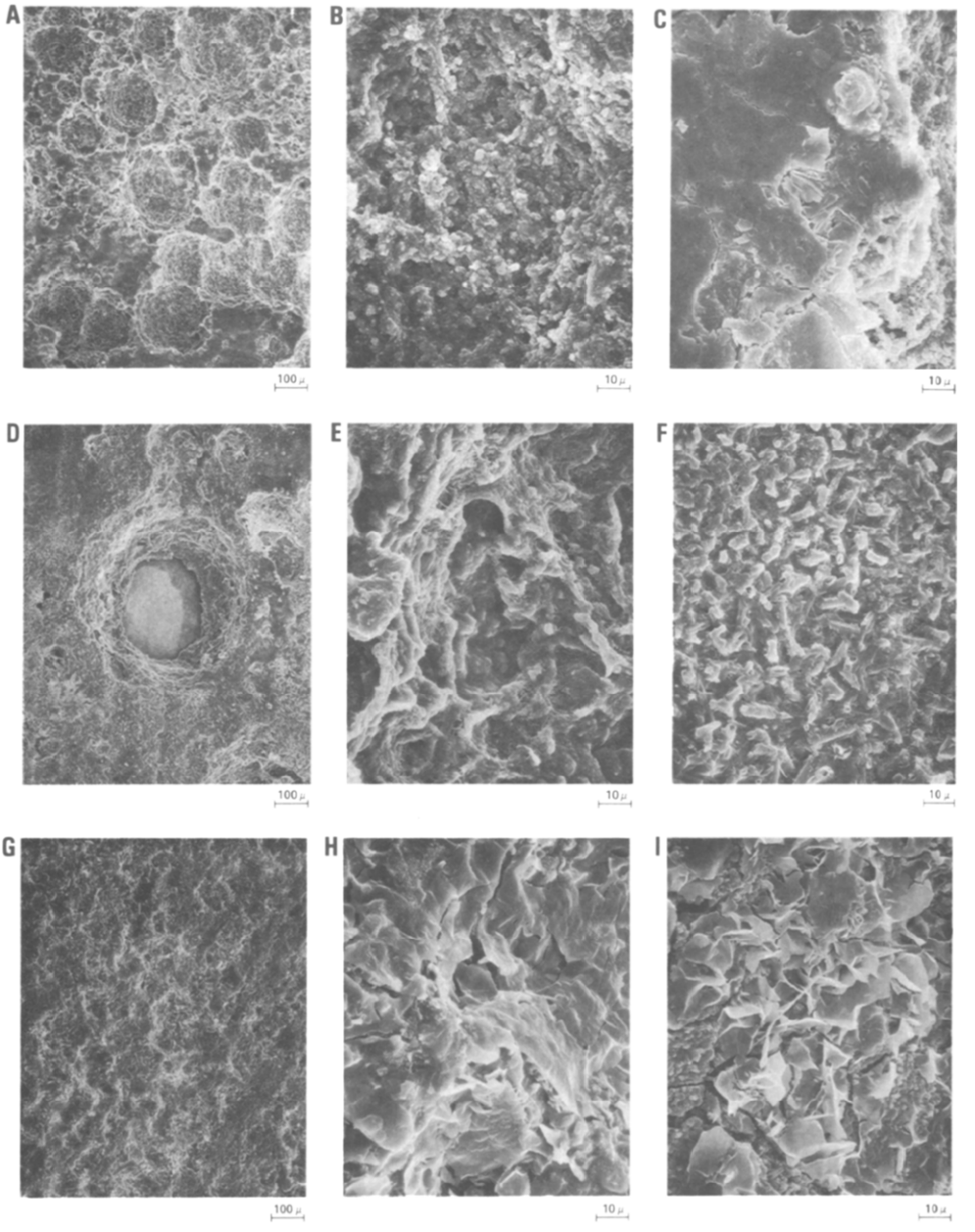

Fig. 1. SEM photomicrographs of discharged anode surfaces. (A) - (C) Anode discharged at −30 °C. (D) - (F) Anode discharged at 24 °C. (G) - (I) Anode discharged at 70 °C.

At −30 °C, the crater formation was observed to result in more numerous but smaller craters (Fig. 1(a)) than those formed at 24 °C during discharge. The surface area in these craters was much larger, however (Fig. 1(b)). This high surface area may help to explain (or merely to be consistent with)

the fact that the Li/SO_2 battery retains relatively good capacity at low temperature. In Fig. 1(c), the thin and largely flat film at the left side is the chemically formed passive layer. To the right is a crater edge and it can be seen that the crater is expanding by undermining the chemically formed passive layer. The thin, chemically formed layer is highly fragmented along several channels and many of these thin, fragmented plates appear much brighter than the surrounding film not yet undermined.

At 70 °C, the effect of discharge is to expand the substrate layer on which the initially continuous chemically-formed passive layer is supported. A widespread system of cracks develops and little or no cratering occurs, as seen in Fig. 1(g). Nodular reaction layer products generally appear in the cracks. A particularly disturbed region is seen in Fig. 1(i), in which the remains of the chemically passivated layer are greatly tossed about. This film thickness is about 0.25 μm in this region, while the anodically formed passive layer appears thicker.

Mass spectroscopy

The mass spectroscopy results on the undischarged lithium anode supply direct evidence for the presence on the anode, or evolution from the anode, of H_2, H_2O, S, H_2S, $LiOCH_3$, CO_2, SO, LiOH, and LiHS. The anode discharged at −30 °C evolves a higher amount of OH species initially, upon pumping on it, which is much larger than the H_2O peak. Peaks attributed to LiO, Li_2O, S and H_2S were also observed. Heating the sample to 120 °C resulted in a tremendous evolution of H_2O. By contrast, the 70 °C discharged anode yields much less H_2O and many more hydrogen-bearing compounds, such as LiHS and H_2S. Unlike the undischarged anode neither of these discharged anodes yielded large amounts of CO_2 or SO.

XPS

A low resolution, broad energy XPS spectrum of the argon sputtered lithium anode discharged at 24 °C is shown in Fig. 2. The initial surface (before sputtering) was exposed to the battery electrolyte for 15 - 30 min after discharge before the battery was disassembled under argon. It was then further exposed to reactions with the residual active gases of glove boxes and less than ultra-high vacuum conditions during transfer. Since the XPS technique probes only the top 30 - 50 Å at the surface, the XPS spectrum of the unsputtered surface cannot be expected to be completely representative of the passive film which is formed anodically, that, is, during discharge. The spectrum of the sputtered surface of Fig. 2 does, indeed, differ from that of the initial surface. The major difference is that there is much more bromine (LiBr) in the anodically formed passive layer compared with that of the passive film chemically formed before or after discharge. Sputtering also removes some carbon (largely in the form of hydrocarbons) which is frequently a contaminant on outer surfaces. Also, sputtering revealed fluorine of the order of 1 at.% (presumably from the Teflon binder in the carbon current collector) which was incorporated into the anodic passive film.

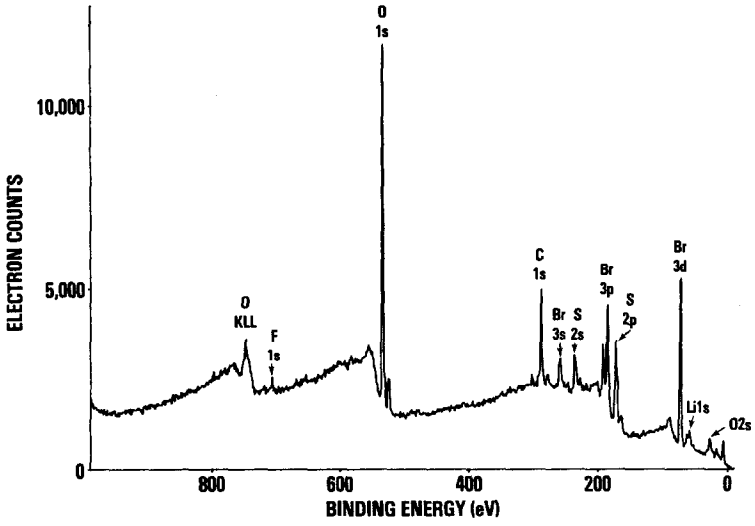

Fig. 2. XPS spectrum of the sputtered anode discharged at 24 °C.

TABLE 2

Lithium anode elemental compositions*

Element	Undischarged		Discharged at 24 °C	
	Surface	Sputtered	Surface	Sputtered
Lithium	29.8%	39.0%	26.9%	34.4%
Sulfur	15.3	15.3	10.9	8.4
Oxygen	43.3	41.1	38.0	38.3
Bromine	1.0	0.8	1.4	5.5
Carbon	10.6	3.7	22.5	13.4
Nitrogen	—	0.1	0.4	—
% S by valence (very approx.)				
+6	56	39	37	50
+4	27	34	53	40
+3,2,1	17	9	4	1
0	0	9	3	5
−2	0	9	3	3

*Elemental composition error is ±20% of stated value.

Table 2 presents the results of calculations of the atomic composition of the cell discharged at 24 °C, and of the undischarged lithium anodes, along with a very approximate breakdown of the sulfur valence state as a percentage of the total sulfur. The elemental composition was determined by finding the area under the high resolution spectra peaks of each element and correcting for the photoionization cross-section, the approximate electron inelastic mean free path, and the energy dependence of the analyzer.

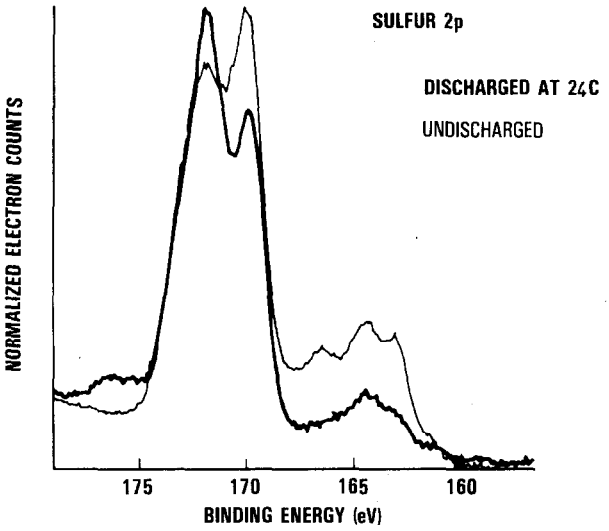

Fig. 3. High resolution XPS sulfur 2p photoelectron spectra of the sputtered undischarged and discharged at 24 °C lithium anodes. These spectra are not corrected, as shown, for the 2 eV charging shift.

Among the many artifacts which can be introduced by ion bombardment of surfaces is the disruption of bonds, particularly ionic bonds. Ion bombardment of LiBr and LiF results in the desorption of some Br_2 and F_2, respectively. In view of this, the strong increase in the Br and F in the ion sputtered surface of Fig. 2 is certainly indicative of a real increase of LiBr and LiF in the anodic film. The anodic passive film is also less rich in sulfur.

Particular interest centers on the complex sulfur chemistry of the electrodes of the Li/SO_2 battery system. High resolution spectra of the normalized sulfur 2p photoelectrons emitted from sputtered undischarged and discharged at 24 °C anodes are compared in Fig. 3. The largest peak of the discharged spectrum is the +6 valence state sulfur. After correcting for sample charging the binding energy is in good agreement with an Li_2SO_4 standard, and it appears to be due predominantly to that compound. The next peak to lower binding energy is a +4 valence state sulfur and is, at least largely, identified as Li_2SO_3 upon comparsion with a standard. The +3 valence state lies generally in the hollow before the next major peak of the undischarged anode and on the falling edge of the +4 valence peak. There is little, if any, lithium dithionite before or after sputtering in either anode. This is consistent with our earlier study of the $LiAsF_6$ salt reserve Li/SO_2 battery system [6]. The third peak to lower binding energy on the sputtered undischarged spectrum is a +1 or +2 valence state and is due to an as yet unidentified compound. The unsputtered, undischarged surface has a strong peak just to the higher binding energy side of this last peak which is due clearly to +2 valence sulfur. The high energy side of the next to lowest binding energy peak on the undischarged anode spectrum of Fig. 3 is due to

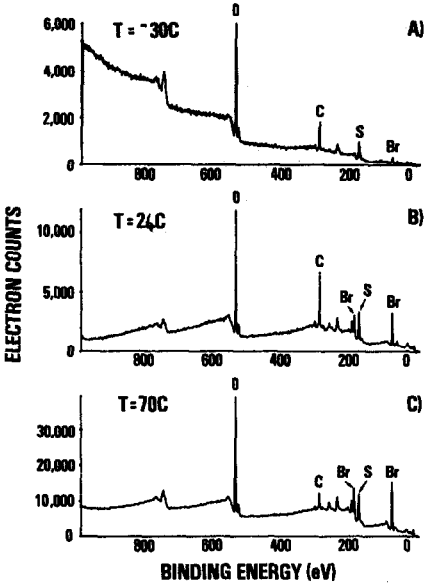

Fig. 4. Comparative XPS spectra for the as-transferred surfaces of the lithium anodes as a function of discharge temperature. (A) −30 °C, (B) 24 °C, (C) 70 °C.

neutral sulfur and the lower side is attributed to LiHS. Mass spectroscopy indicated the presence of both, and the peak identification results from observing XPS peak changes as a function of sample heating correlated with the mass spectrometry results. The final peak is due to lithium sulfide and corresponds well with an Li_2S standard.

The initial surface spectrum of each showed much less S, LiHS, and Li_2S in the undischarged case and none in the room temperature discharged case. This may be partly due to their very great reactivity with active residual gases. The initial surface of the undischarged anode had a strong +2 valence state sulfur peak. It was only this surface which yielded a strong SO peak in the mass spectroscopy study, as well. The initial surface of the undischarged anode was primarily about equally Li_2SO_4 and Li_2SO_3, whereas that of the discharged at 24 °C surface was almost entirely Li_2SO_3.

Comparative broad energy spectra for the −30, 24, and 70 °C discharges are given in Fig. 4. The −30 °C discharge spectrum was made in an analyzer mode for which the transmission is inversely proportional to the kinetic energy rather than directly proportional, as are the others. These, and high resolution spectra of the initial surfaces, clearly show a trend toward increased incorporation of LiBr in the anodic passive film and a decrease in the sulfur compounds. After sputtering, the ratio of Br to S increases in each case, which is contrary to the undischarged case. This is the more remarkable since some extra LiBr is precipitated on the unwashed anode surfaces. The same trend toward more LiBr at higher temperatures is then also seen. At 70 °C there is a doubling of the low valence sulfur compounds relative to the

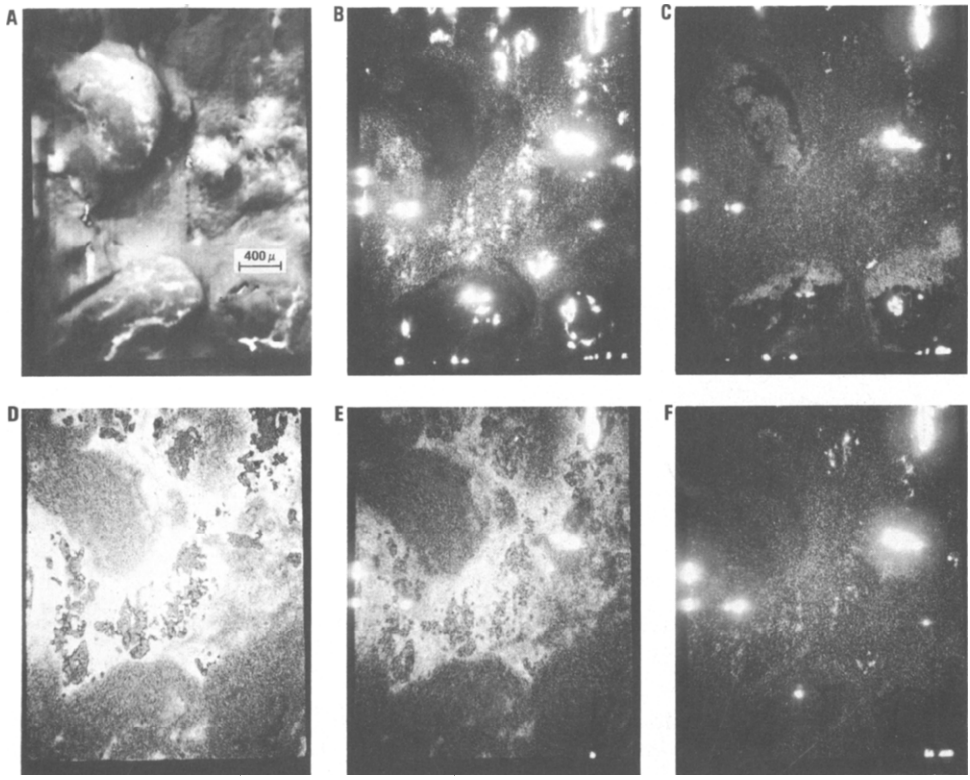

Fig. 5. SAM photomicrographs of the same region with identical beam resolution of an anode discharged at 70 °C. (A) Total secondary electron map. The following photos are Auger electron maps of (B) lithium (35 eV), (C) lithium (47 eV), (D) oxygen (507 eV), (E) sulfur (147 eV), (F) bromine (95 eV).

+6 and +4 valence states and no +2 valence state is seen before or after sputtering. During −30 °C discharge, no low valence sulfur compounds form except for the +2 valence state which is observed both before and after ion bombardment.

It must be noted that we observe ion-bombardment-induced chemical changes upon sputtering bulk samples of Li_2SO_4, Li_2SO_3, and Li_2S. Complex redistributions between these compounds occur, but these redistributions do not obscure the general trends we have outlined above under the sputtering conditions used here. An XPS study of ion bombardment damage of transition metal sulfates [7] also gives some reason for caution, despite apparent differences of mechanism for the lithium salts.

SAM

Just as the SEM electron photomicrographs reveal strong microstructural inhomogeneities across the surface of discharged lithium anodes, so too do the SAM elemental Auger electron photomicrographs show strong chemical inhomogeneities. Figure 5 gives the secondary electron map of the same

region for which the Li, O, S, and Br elemental Auger maps are given for the anode surface discharged at 70 °C. These maps were made using a 3 keV electron beam at 50 nA. Visible beam damage occurred if the beam was allowed to sit at a spot for a minute or two, so the beam was continually rastered with the result that little observable beam damage occurred in the course of making these photomicrographs. Electron beam damage effects on bulk Li_2SO_4 have been studied elsewhere [8]. The brighter the area, the higher is the concentration of the element in question. Two lithium maps are given since the prominent Li Auger peaks in different Li compounds differ in energy. Areas rich in oxygen, but only moderately so in lithium and sulfur, are regions of higher Li_2SO_4 and Li_2SO_3 concentrations. Regions high in both Li and S are Li_2S and LiHS. Those high only in S are neutral sulfur. Those high only in Li and Br are predominantly LiBr, while those high in Li and O are Li_2O or, more likely, LiOH. Those few and small regions high only in Li are expected to be LiH, which we have found in large quantity in the 70 °C discharge carbon current collector.

Acknowledgments

This work was supported by Independent Research Funds of the Naval Surface Weapons Center and the Electrochemistry Technology Block Program of NAVSEA. M. K. Norr is heartily thanked for his SEM artistry. R. N. Lee is gratefully thanked for his support at the Surface Evaluation Facility.

References

1 P. Bro, N. Y. Yang, C. Schlaikjer and H. Taylor, *Tenth IECEC, 1975*, Institute of Electrical and Electronic Engineers, p. 423.
2 D. Linden and B. McDonald, *J. Power Sources, 5* (1980) 35.
3 A. N. Dey, *Thin Solid Films, 43* (1977) 131.
4 W. P. Kilroy, *Talanta, 27* (1980) 343.
5 D. M. Oglesby, R. L. Ake and W. P. Kilroy, *Proc. 30th Power Sources Symp., Atlantic City, NJ, June, 1982*, The Electrochemical Society, Princeton, NJ.
6 C. R. Anderson, S. D. James, W. P. Kilroy and R. N. Lee, *Appl. Surf. Sci., 9* (1982) 388.
7 G. J. Coyle, T. Tsang, I. Adler, N. Ben-Zvi and L. Yin, *J. Electron Spectrosc. Relat. Phenom., 24* (1981) 221.
8 T. Sasaki, R. S. Williams, J. S. Wong and D. A. Shirley, *J. Chem. Phys., 68* (1978) 2718.